International Journal of Applied Pharmaceutics

ISSN- 0975-7058 Vol 16, Issue 1, 2024

Original Article

REVOLUTIONIZING THERAPEUTIC DELIVERY: DIOSGENIN-LOADED SOLID LIPID NANOPARTICLES UNLEASH ADVANCED CARRIERS

RAMSHA ASLAM[1,2*], VARSHA TIWARI[3], PRASHANT UPADHYAY[4], ABHISHEK TIWARI[3]

[1]Faculty of Pharmacy, IFTM University, Lodhipur-Rajput, Moradabad-244102, Uttar Pradesh, India. [2]Devsthali Vidyapeeth College of Pharmacy, Lalpur, Rudrapur, U. S. Nagar, India. [3]Pharmacy Academy, IFTM University, Lodhipur-Rajput, Moradabad-244102, Uttar Pradesh, India. [4]School of Pharmaceutical Sciences, IFTM University, Lodhipur-Rajput, Moradabad-244102, Uttar Pradesh, India
***Corresponding author: Ramsha Aslam; *Email: ramshaaslam061990@gmail.com**

Received: 06 Sep 2023, Revised and Accepted: 11 Oct 2023

ABSTRACT

Objective: The pharmaceutical industry has paid a lot of attention to solid lipid nanoparticles (SLN) because they show promise as drug delivery vehicles. The purpose of this research was to create and characterize SLN loaded with Diosgenin.

Methods: To create SLN, the natural bioactive component diosgenin was encapsulated in a solid lipid matrix of compritol ATO 888. A modified solvent emulsification-evaporation process was used to create the SLN. Using a Box-Behnken Design (BBD), we were able to identify the optimal values for the drug-to-solid lipid ratio, surfactant concentration, and ultrasonication period that constitute an effective formulation.

Results: It was found that the improved formulation had particle sizes of 170.96 nm, polydispersity indices (PDI) of 0.231, and entrapment efficiencies of 64.549±0.553% %. The zeta potential value of -40.2 mV was indicative of a steady dispersion. The average particle size of the SLN was measured to be 103.1429 nm, and their spherical morphology was validated by scanning electron microscopy (SEM) imaging. The optimized formulation did not undergo any chemical changes, as shown by differential scanning calorimetry (DSC) testing. The *in vitro* drug release investigation showed that the SLN released Diosgenin continuously for 28 h.

Conclusion: The optimized formulation of SLN, achieved through the BBD, offers a promising strategy to improve drug solubility while ensuring controlled drug release and long-term storage stability.

Keywords: Diosgenin, Solid lipid nanoparticles, Formulation optimization, Drug release, Bioactive compound

DOI: https://dx.doi.org/10.22159/ijap.2024v16i1.49306 Journal homepage: https://innovareacademics.in/journals/index.php/ijap

INTRODUCTION

The successful delivery of drugs to their target sites within the body is crucial for achieving desired therapeutic outcomes. However, many drugs suffer from poor solubility, low bioavailability, rapid metabolism, and elimination, leading to suboptimal therapeutic efficacy. To overcome these challenges, the development of suitable drug delivery systems is imperative. In recent years, SLN has emerged as a promising class of lipid-based colloidal carriers for enhancing the solubility and delivery of hydrophobic drugs. SLN are sub-micron-sized particles with a range of 50 to 1000 nm, composed of physiological lipids dispersed in an aqueous surfactant solution. These nanoparticles offer several advantages over traditional drug carriers, including high biocompatibility, improved drug stability, increased bioavailability, enhanced targeting capabilities, and the ability to be produced in large quantities [1, 2]. The encapsulation of the drug into the SLN increases the availability of the drug at the site of action as shown in fig. 1. By encapsulating the drug within SLN, several advantages are achieved. Firstly, the SLN protects the drug from degradation or premature release, thereby prolonging its circulation time in the body. This extended circulation time allows for increased drug accumulation at the target site. Secondly, the small size of SLN facilitates their passive targeting of specific tissues or cells due to the enhanced permeability and retention (EPR) effect. The SLN can passively accumulate in areas with compromised vasculature, such as tumor tissues, leading to higher drug concentrations at the site of action [2].

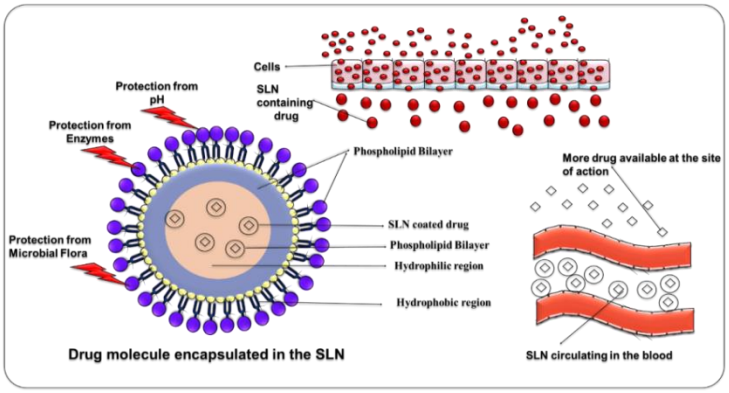

Fig. 1: The encapsulation of the drug in the SLNs increases the availability of the drug at the site of action (Source: Authors)

Diosgenin is a steroidal sapogenin that is found in large amounts in Dioscorea alata, *Trigonella Foenum graecum*, and Smilax China [3]. This bioactive plant chemical has shown a lot of promise and interest in treating diseases like cancer, diabetes, problems from diabetes, high cholesterol, inflammation, and several types of infections [4, 5]. Still, diosgenin's main problems for clinical use are

that it doesn't mix well with water and that it isn't very effective when taken by mouth [6, 7]. Because of these problems, diosgenin is a great example of a lipophilic drug for SLN and NLC to learn from. The development of diosgenin SLN could have big effects on patient care [8].

The goal of this study was to use a randomized response surface BBD to make and improve SLN loaded with diosgenin. The exact goals were to make the drug more soluble, get a steady release of the drug, and make sure the formulation is stable over time. The melt emulsification-ultrasonication method was used to make SLN because it is easy and can be used on a large scale. First, different lipids were tested to see how well they mixed with diosgenin. Compritol ATO 888 was found to be the best lipid, and further tuning was done using a BBD, taking into account things like the amount of solid lipid, the amount of surfactant, and the amount of time spent sonicating. With a response surface method [9, 10], the effects of these independent variables on particle size, polydispersity index (PDI), and entrapment efficiency were looked at. A lot of information was gathered about the best way to make diosgenin-loaded SLN. To fig. out what the nanoparticles were made of and how stable they were, their particle size, PDI, and zeta potential were measured. SEM was used to look at the shape and surface morphology of the SLN, and DSC was used to look at the interactions between the drug and lipids in the mixture [11, 12]. Using a dialysis bag method, drug release studies were done in the lab. Drug release rates were measured in both acidic and phosphate buffer environments. Using different models, such as the zero-order, first-order, Korsmeyer-Peppas, Higuchi, and Hixson-Crowell models [13, 14], the release dynamics of the optimized formulation were studied. Last, stability studies were done to find out how long the optimized formulation would stay stable under different storage situations. Over 30 d, the size of the particles and how well they were caught were watched to see if there were any noticeable changes [15]. So, the developed SLN with the optimized formulation offers a hopeful way to make drugs more soluble, get a steady release of drugs, and make sure that diosgenin stays stable for a long time. These results have important implications for making diosgenin more effective as a medicine and for using it in the clinic to treat different diseases.

MATERIALS AND METHODS

Materials

The phytoconstituent Diosgenin was procured from Yarrow Chem, Mumbai, India. Compritol ATO 888 and Phospholipon® 80H were purchased from HiMedia, Rudrapur, India, while Tween 80 was procured from Finar, Ahmedabad, India.

Screening of lipids

Due to the solid structure of lipids, it is difficult to determine the solubility of diosgenin using the equilibrium approach, as described by Das *et al.* (2011). The drug and lipids were combined in two different drugs: lipid ratios of 1:2 and 1:3. The resulting mixture was uniformly mixed for 5 min while melting at 5 °C above the lipid MP. Samples were checked visually for clarity and miscibility [16, 17].

Experimental design

In this study, the effects of three independent variables on the size (nm) and percent entrapment of SLN were investigated using a response surface approach. The independent variables considered were the amount of solid lipid (mg), sonication time (min), and surfactant quantity (percent). To conduct the experiments, a randomized response surface BBD was employed, which allowed for the creation of seventeen different combinations of the independent variables. Each variable was assigned three levels: -1, 0, and 1 given in table 1. The experimental design was randomized, and the tests were performed in a random order.

To establish a relationship between the coded and uncoded values of the independent variables, Equation (1) was utilized. In this equation, X represents the coded level, X_0 corresponds to the real level of the independent variable, ΔX denotes the step change, and X_C represents the actual value at the central point. The equation enabled the conversion between coded and uncoded data.

X_1= Solid lipid, X_2= Surfactant concentration, X_3 = Sonication time

$$X = X_0 - \frac{X_C}{\Delta X} \quad \ldots\ldots\ldots\ldots\ldots\ldots (1)$$

A non-linear polynomial equation derived from the BBD, was employed to model the relationship between the independent variables and the response (Y). The equation ($Y = b_0+b_1X_1+b_2X_2+b_3X_3+b_{12}X_1X_2+b_{13}X_1X_3+b_{23}X_2X_3+b_{11}X_1^2+b_{22}X_2^2+b_{33}X_3^2$) consisted of an intercept term (b_0), linear coefficients (b_1, b_2, b_3), interaction coefficients (b_{12}, b_{13}, b_{23}), and quadratic coefficients (b_{11}, b_{22}, b_{33}). These coefficients were determined based on the observed experimental values of the responses obtained from the experimental runs. The independent variables X_1, X_2, and X_3 represented the coded values of the solid lipid, surfactant concentration, and sonication time, respectively [18, 19].

Table 1: Independent and dependent variables and their levels in BBD

Independent variable	Symbol	Coded level		
		-1	0	+1
Drug: solid lipid	X_1	1:3	1:4	1:5
Surfactant %	X_2	2	3	4
Sonication (min)	X_3	6.0	7.5	9.0

Fabrication of solid lipid nanoparticles

SLN was made using a modified method of melt emulsification and ultrasonication. After looking at lipids, Compritol ATO 888, which has a melting point of 70 °C, was picked as a solid for the synthesis of SLN. The solid lipid was melted at a temperature that was 10 degrees Celsius above its melting point. The drug was then added slowly while the mixture was constantly stirred. This made the liquid phase [20, 21]. The lipid phase and the water phase were both heated to the same temperature. The water phase had Tween 80 as a detergent and Phospholipon® 80H (1 percent w/v) as a stabilizer. To make a pre-emulsion, the watery phase was slowly added to the oily phase while shaking at the same temperature. The hot pre-emulsion was then shaken with a sonicator. The heated, uniform pre-emulsion was ultrasonicated with a probe sonicator (PCI Analytics) with a 20:2 on/off cycle [22, 23]. The o/w nanoemulsion that was made was left to cool to room temperature so that the lipid phase could recrystallize and help make SLN. By using a High-speed cooling centrifuge (REMI), the unbound medicine in the SLN aqueous mixture was taken out [24, 25].

Characterization of diosgenin-loaded SLN

Size distribution and polydispersity index study

Photon correlation spectroscopy (PCS) with a zeta sizer at a set angle was used to fig. out the average diameter and PDI of the made formulation. Before measuring the size of the particles, the material was broken up ten times in distilled water [26, 27]. The mean diameter and PDI of the samples under study were found by taking the average of three measures. All of the tests were done when it was 25 degrees Celsius outside [28-30].

Determination of entrapment efficiency

After being diluted with methanol and put through a centrifuge, the diosgenin that had not been encapsulated was able to be separated [31, 32]. After passing through a filter, the supernatant was subjected to spectrophotometric analysis at 206 nm using the same solvent as was used for the blank [33, 34]. The encapsulation efficiency percentage, also known as the EE percent, was found by using the following equation to solve the problem [35, 36].

$$\% \text{ Entrapment efficiency} = \frac{\text{Total amount of drug} - \text{Amount of drug unentrapped}}{\text{The total amount of drug}} X\ 100$$

Zeta potential analysis

The electrophoretic mobility of the SLN dispersion was evaluated with the help of the Malvern Zetasizer, and the zeta potential of the dispersion was computed [37, 38]. The measurements of each sample were performed three times [39, 40].

Differential scanning colorimetry

To explore the phase transition features and the impact of thermal changes on the physical state of the sample, a DSC analysis was performed on the created nano-formulation using a conventional approach. DSC (Perkin-Almer) was used to compare the pure drug, the pure Compritol ATO 888, the physical mixing of drug and lipid, and the optimal formulation of drug-loaded SLN in the scanning range of 30-300 °C, holding period 1 min at 30 °C, and heating rate 30 °C/min [41, 42].

Shape and surface morphology

The morphology of the optimized diosgenin-loaded SLN formulation was analyzed using SEM [43-46].

***In vitro* release**

In vitro drug release tests were performed on the optimized batch at a temperature of 35.5 degrees Celsius using a dialysis bag technique with a dialysis membrane for the first two hours in 0.1N HCl and then for an additional up to 28 h in phosphate buffer pH 6.8 [47, 48]. After being accurately weighed out, diosgenin-loaded SLN dispersions were put into a dialysis bag and then the bag was put into use. Following that, the bag was placed inside a beaker that contained 250 milliliters of a physiological solution [43, 49]. At various time intervals of 2, 3, 4, 5, 6, 24, and 28 h, 1 milliliter of the receptor phase was removed and replaced with an equal volume of new fluid. A UV spectrophotometer set at 206 nm was used to evaluate each of the samples.

Drug release kinetics

The data on drug release was mathematically processed using the zero-order model, the first-order model, the Higuchi diffusion model, and the Korsmeyer-Peppas model so that the drug release mechanism could be described [50-53].

Stability

The stability tests were carried out for a whole month at temperatures ranging from 2 to 8 degrees Celsius and at relative humidities of 60 percent [54].

RESULTS

Screening of lipids

The solubility-based screening of solid lipids suggested the best solid lipid for the creation of drug-loaded SLN is Compritol® 888 ATO. As shown in table 2, The solubility of diosgenin in melted Compritol 888 ATO was maximum.

Table 2: Solubility study

Lipid	MP	Diosgenin: lipid		Remark
		1:2	1:3	
Precirol ATO 5	52-35	Opaque	Turbid	Not suitable for SLN
Glycerol monostearate	55-60	Opaque	Opaque	Not suitable for SLN
Stearic acid	69-70	Opaque	Opaque	Not suitable for SLN
Compritol ATO 888	65-77	Turbid	Clear	suitable for SLN

Data analysis and optimization of diosgenin-loaded SLNs

BBD was used for process optimization with three levels and three factors. There are 17 runs of various combinations, which are given in table 3. To choose the most effective experimental parameter, all the observed responses were compared and evaluated. ANOVA (analysis of variations) was used to analyze the data and predict the most effective mathematical model (table 4).

Table 3: BBD matrix with transformed values and the measured responses

		X_1	X_2	X_3	Response 1		Response 2	
Std	Run	Drug: solid lipid ratio	Surfactant concentration	Ultrasonication time	Size observed	Size predicted	Entrapment efficiency observed	Entrapment efficiency predicted
			%	Min	nm	nm	%	%
16	1	0	0	0	260.12	258.22	67.23±1.76	66.40
5	2	-1	0	-1	175.03	175.00	51.27±0.54	51.25
6	3	1	0	-1	375.21	378.25	53.37±0.49	53.25
13	4	0	0	0	251.13	258.22	66.34±0.32	66.40
1	5	-1	-1	0	170.06	171.62	65.51±0.51	64.75
8	6	1	0	1	370.07	370.00	58.07±0.26	57.75
3	7	-1	1	0	190.11	191.63	63.08±0.79	63.25
14	8	0	0	0	259.13	258.22	65.47±0.64	66.40
11	9	0	-1	1	280.24	281.63	56.66±0.89	56.50
10	10	0	1	-1	305.31	303.38	51.54±0.32	50.50
2	11	1	-1	0	370.26	368.37	67.29±0.55	66.75
17	12	0	0	0	261.1	258.22	67.12±0.37	66.40
15	13	0	0	0	259.98	258.22	67.17±0.66	66.40
4	14	1	1	0	390.01	388.37	65.15±0.27	65.25
7	15	-1	0	1	183.19	179.75	56.31±0.86	55.75
12	16	0	1	1	300.12	301.63	54.32±0.64	54.00
9	17	0	-1	-1	285.26	283.38	51.56±0.58	51.00

*% Entrapment efficiency n=3, (mean±SD)

Effect of independent process variables on particle size

The results showed that all of the produced formulations have particle sizes ranging from 170.06 nm to 390.01 nm. The particle size of all the formulations is given in table 03. It is abundantly clear that the drug lipid ratio (X_1) directly affects particle size, whilst an increase in surfactant concentration (X_2) first caused a significant decrease in particle size, followed by a minor increase with

additional increases in surfactant concentration. Initial surfactant concentration increases were intended to lower interfacial tension, generate steric hindrance on the surface of the SLN, limit the accumulation of individual particles, and improve stability.[55]

There was very little impact of ultrasonication time (X_3) on particle size. More thorough information on the impact of numerous independent parameters on particle size is provided by a 3D response surface plot in fig. 2A.

Table 4: Optimization and model validation of diosgenin-loaded SLN

	Source	Sequential p-value	Lack of Fit P-value	Adjusted R^2	Predicted R^2	
Size	Linear	<0.0001	0.0064	0.9563	0.9442	
	2FI	0.9845	0.0033	0.9440	0.8975	
	Quadratic	<0.0001	0.5398	0.9969	0.9904	Suggested
	Cubic	0.5398		0.9967		Aliased
EE	Linear	0.7784	0.0003	-0.1348	-0.6456	
	2FI	0.9994	0.0002	-0.4729	-2.5470	
	Quadratic	<0.0001	0.7510	0.9859	0.9691	Suggested
	Cubic	0.7510		0.9812		Aliased

The R^2 value is near to it estimated that the object response is near the estimated response, which shows that our method is validated for the preparation.

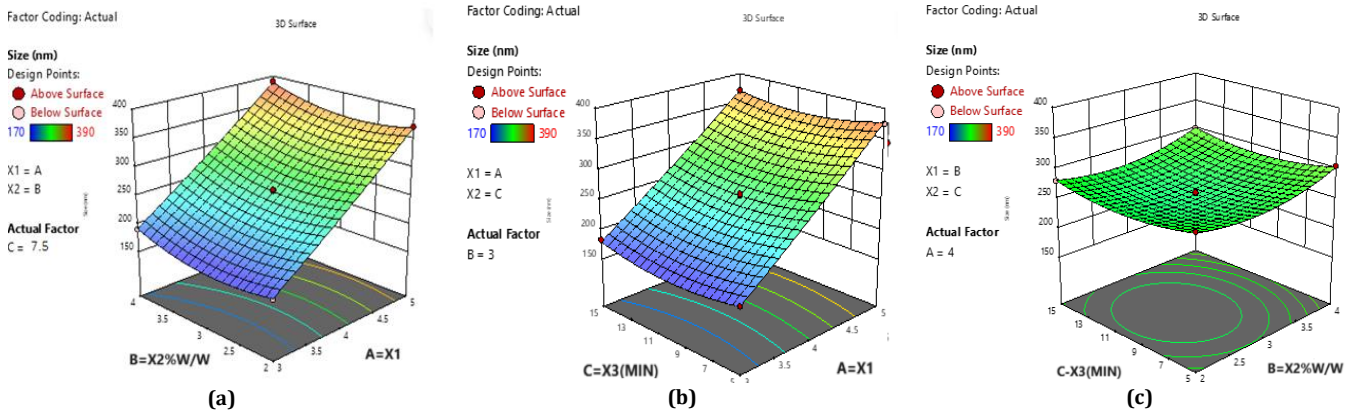

Fig. 2A: 3D graphic surface plot for optimization of prepared SLN-(A-C) represents the effect of X_1, X_2, and X_3 on particle size

Effect of independent process variables on encapsulation efficiency

The results showed that all of the produced formulations (n=3) have entrapment efficiency ranging from 51.27±0.54-67.23±1.76%. The entrapment performance of all the formulations is given in table 3. According to the 3D response surface graphs, the increased ratio of drug and lipid somewhat increases the formulation's entrapment efficiency (X_1). This might be because the lipid content has increased, aiding in the drug's solubilization. The entrapment efficiency initially increased with surfactant content(X_2) and ultrasonication time(X_3) before beginning to deteriorate. The drug partitioning in both the lipid and aqueous phases may be improved by an increase in surfactant concentration. Further addition of surfactant is responsible for drug expulsion from the matrix, so decreased entrapment efficiency was observed. However, the use of ultrasonication initially promoted the transfer of drug molecules from the aqueous phase to the matrix and promoted drug entrapment, while a further extension of the sonication time may result in drug ejection from the matrix [55]. More thorough information on the impact of numerous independent parameters on entrapment efficiency is provided by a 3D response surface plot in fig. 2B.

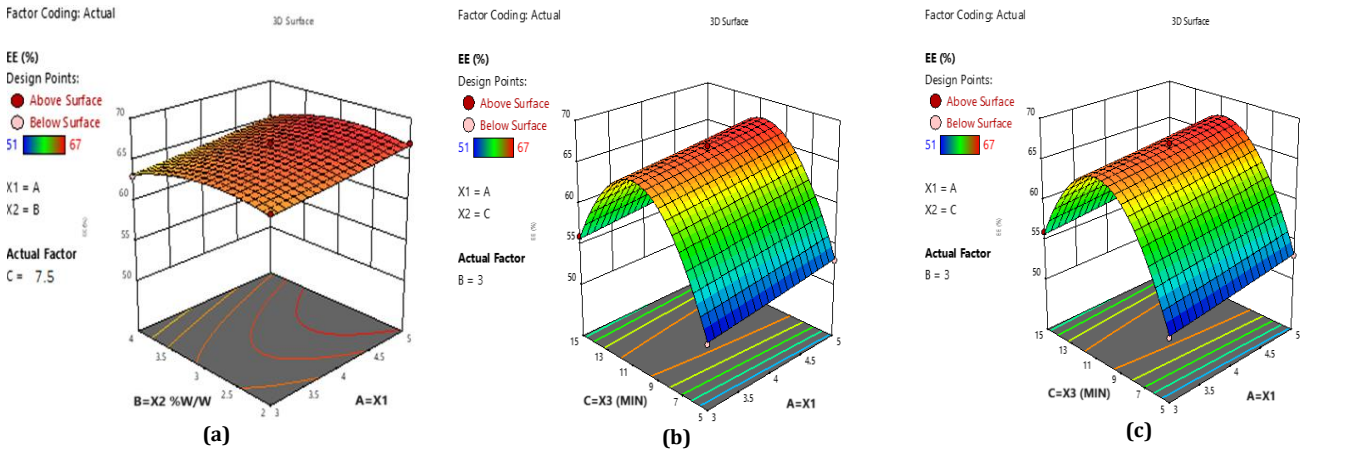

Fig. 2B: 3D graphic surface plot for optimization of prepared SLN-(A-C) represents the effect of X_1, X_2, and X_3 on entrapment efficiency

Optimization

Statistical examination and by determining the effect of independent factors on responses, the optimized formulation parameters were selected by software. BBD recommended the most suitable numeric values for the preparation of optimized formulation as 3.90 Drug: Solid lipid ratio, 2.642% surfactant concentration, and 7.58 min ultrasonication time. The optimized formulation was then subjected to further studies [55].

Characterization of diosgenin-loaded SLN

Particle size, PDI, and entrapment efficiency

The particle size of the optimized diosgenin-loaded SLN was found to be 170.96 nm. This indicates the successful formation of nanosized particles, which is beneficial for drug delivery applications. Nanoparticles in this size range have been shown to improve drug delivery efficiency, increase cellular uptake, and enhance bioavailability due to their small size and increased surface area. The low PDI value of 0.231 further confirms the homogenous distribution of particles within the formulation. A low PDI indicates minimal aggregation and narrow size distribution, which is crucial for the stability and reproducibility of the SLN [56, 57]. The particle size graph of the optimized formulation is given in fig. 3.

The high entrapment efficiency of 64.549±0.553% for diosgenin in the optimized SLN is a significant finding. Entrapment efficiency represents the percentage of drug incorporated within the nanoparticles during the formulation process. A high entrapment efficiency suggests that a large proportion of the drug is successfully encapsulated within the lipid matrix, preventing drug leakage and degradation and enhancing the potential therapeutic efficacy [58, 59].

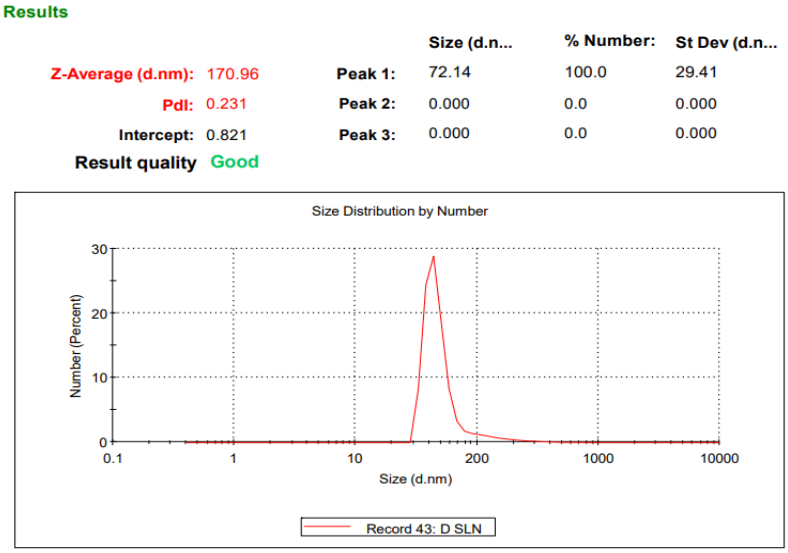

Fig. 3: The particle size of the optimized formulation

Zeta potential analysis

The stability of colloidal dispersion depends on the magnitude of the surface charge. The zeta potential value of the optimized formulation was found to be-40.2 Mv, which indicates the stability of dispersion without aggregation. This negative charge contributes to the electrostatic repulsion among particles, preventing their aggregation and ensuring the long-term stability of the colloidal dispersion [60]. The zeta potential graph of the optimized formulation is given in fig. 4.

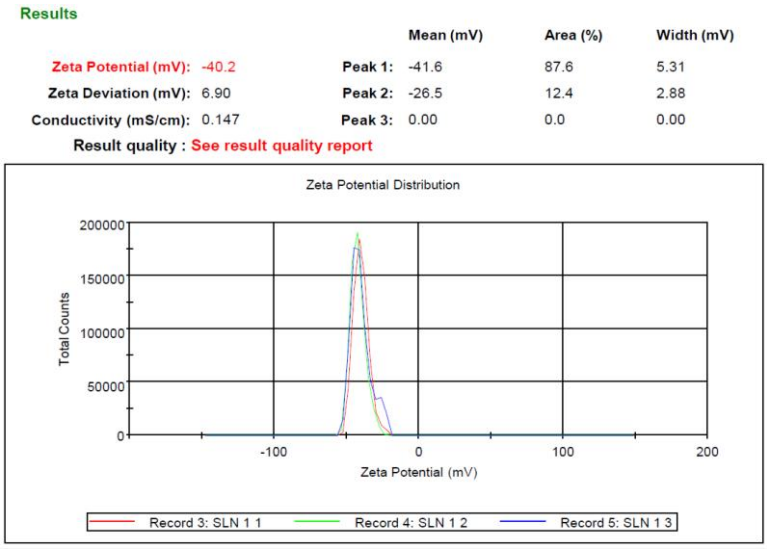

Fig. 4: Zeta potential of diosgenin-optimized formulation

Differential scanning colorimetry

The thermogram of diosgenin pure and compritol ATO 888 pure showed a sharp peak at 210 °C (fig. 5a) and 72 °C (fig. 5b), respectively. A physical mixture of diosgenin and compritol ATO 888 showed a sharp peak at approximately 190 °C (fig. 5C) due to the exchange of heat, but a sharp peak indicates no chemical changes. DSC of optimized formulation showing broadband (fig. 5D) due to the interaction of drug and other formulation ingredients. These interactions may contribute to the enhanced solubility and controlled release of diosgenin from the SLN, making it a potential strategy to improve the drug's bioavailability [61-63].

Shape and surface morphology

The diosgenin-loaded SLNs' best composition was looked at with SEM. The particles were round and their sizes ranged from 84.09735 to 122.1884 nm as shown in fig. 6. The average size of the particles was found to be 103.1429 nm.

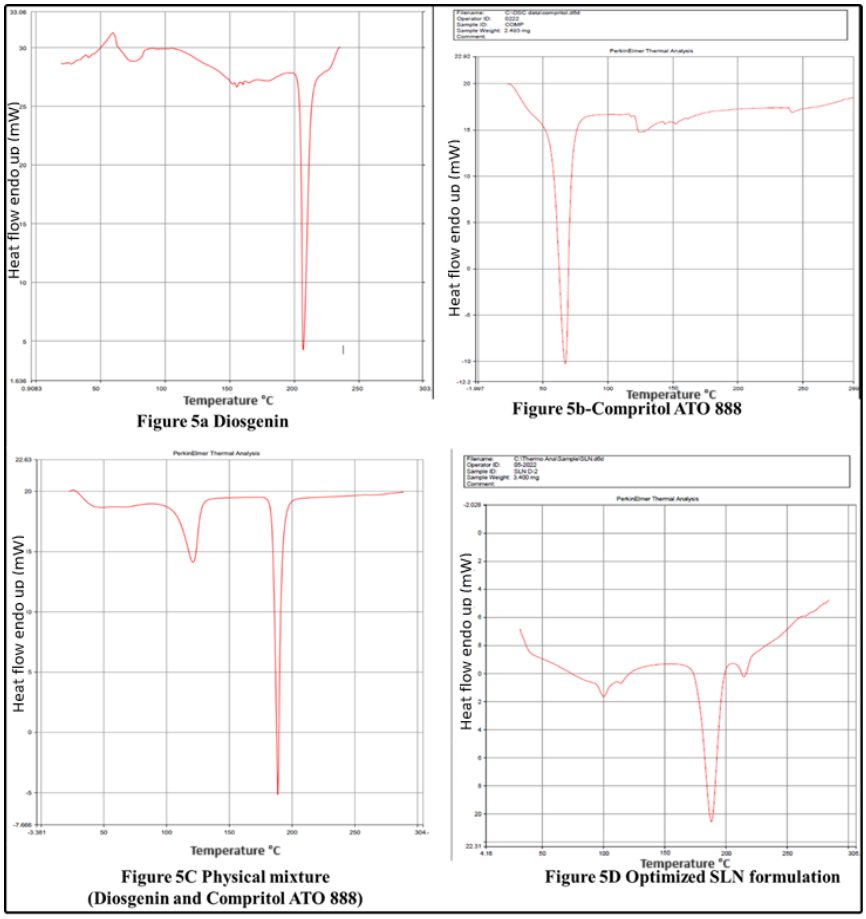

Fig. 5: DSC thermogram of (A) Pure drug, (B) Compritol ATO 888 (C) physical mixture (D) SLN formulation

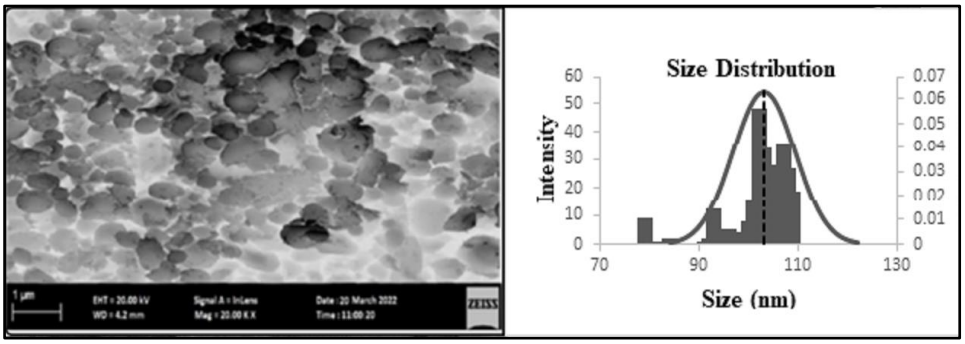

Fig. 6: SEM image and particle size distribution curve of optimized formulation

***In vitro* release**

In vitro drug release from the SLN was studied by dialysis bag technique initially 2 h in 0.1N HCl and further up to 28 h in phosphate buffer pH 6.8. The findings demonstrated that diosgenin is hydrophobic, it shows a maximum of 30.17% of drug release in the whole span of the release profile but the formulation has characteristic release and solubility. Drug release of optimized formulation was 68.27% in 28 h. The sustained release is beneficial for maintaining therapeutic drug concentrations, reducing dosing frequency, and potentially improving patient compliance [64, 65]. The *In vitro* drug release of diosgenin pure and optimized formulation is illustrated in fig. 7.

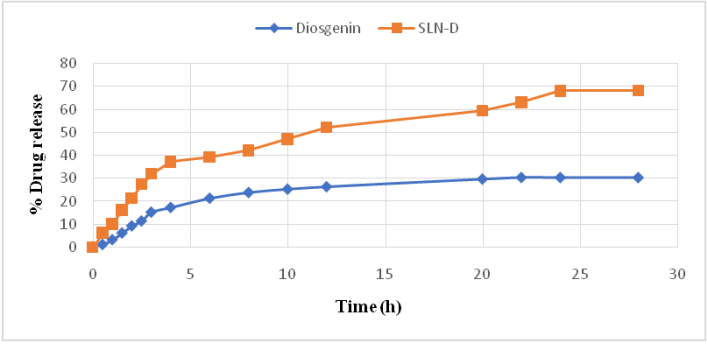

Fig. 7: Comparison of the *in vitro* release of pure diosgenin and optimized formulation

Drug release kinetics

Several alternative kinetic models, including the zero-order model, the first-order model, the Korsmeyer-Peppas model, the Higuchi model, and the Hixson-Crowell model, were used to analyze the drug release profile of the optimized SLN formulation (fig. 8). Based on the value of R^2, the Higuchi model (table 5) is the most well-suited one to reflect the release. According to the available research, the Higuchi model illustrates the release process as a mechanism of diffusion-controlled through a matrix.

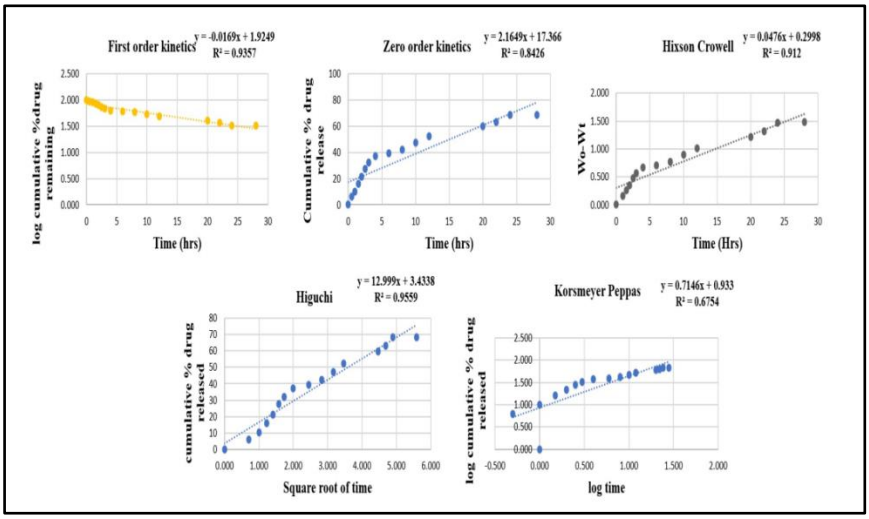

Fig. 8: Drug release kinetics of optimized-formulation

Table 5: R^2 value of different release kinetics model

Models	Zero-order	first-order	Korsmeyer-peppas	Higuchi	Hixson-crowell
R^2	0.8444	0.9357	0.634	0.9559	0.9095

Stability

The robust stability of the diosgenin-loaded SLN over 30 d, with no significant changes in particle size and entrapment efficiency, demonstrates their potential for long-term storage and potential commercialization [66], which is given in table 6. Stability is a critical factor for the successful translation of nanoparticle-based drug delivery systems from the lab to practical applications.

Table 6: Stability studies

Storage condition	Particle size (nm)			Entrapment efficiency (%)*		
	Initial	30 d	90 d	Initial	30 d	90 d
2-8 °C	170.96	173.84	179.67	64.549±0.553	63.85±0.193	63.18±0.155
25 °C/60% RH	170.96	172.17	176.45	64.549±0.553	63.12±0.072	62.76±0.546

*% Entrapment efficiency n=3, (mean±SD)

Possible mechanisms

The diosgenin-loaded SLN revolutionizes drug delivery by tackling the persistent challenge of poor bioavailability in orally administered drugs. These innovative SLN enhance drug solubility, overcome physiological and formulation barriers, and significantly improve drug absorption and availability. By forming micelles with lipids, SLN boosts drug solubility, facilitating its absorption and bioavailability (fig. 9).

They bypass the first-pass effect by being absorbed through lymphatic vessels, ensuring a higher proportion of the drug reaches the systemic circulation. SLN also leverages nanoparticulate systems to enhance drug uptake by M-cells of Peyer's patches and inhibit efflux transporters, further enhancing absorption. With their unique properties, such as steric hindrance and sustained release, SLN offers prolonged drug exposure, maximizing absorption and therapeutic efficacy. This groundbreaking technology opens new possibilities for enhancing oral drug delivery and revolutionizing the treatment of various disorders [67-71].

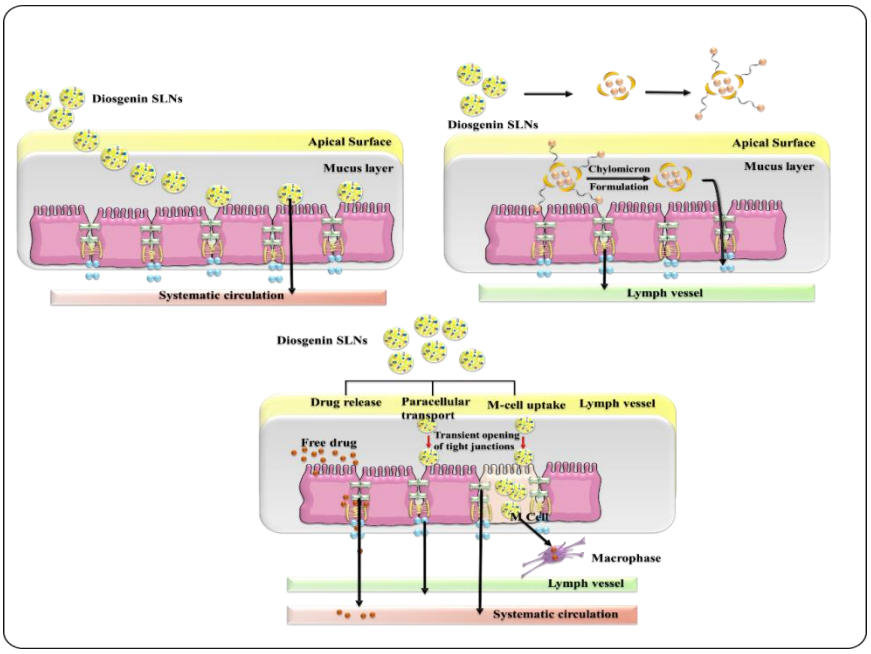

Fig. 9: Possible mechanisms by which diosgenin SLN enhances oral bioavailability

CONCLUSION

The experiment design and optimization were carried out utilizing the response surface approach and BBD in the present study to show how diosgenin-loaded SLN was designed and optimized using a modified melt emulsification procedure followed by ultrasonication. The goal of the project was to develop cost-efficient, biodegradable, stable nanoparticles with increased drug entrapment and a sustained, recognizable release profile by diffusion mechanism. Particle size was 170.96 nm, PDI was 0.231, zeta was -40.2 Mv, and entrapment efficiency was 64.549±0.553% percent in the optimized formulation of SLN. The formed SLN with the optimized formulation obtained via BBD was thought to be a potential approach for enhancing drug solubility with characteristic drug release and long-term storage stability.

ACKNOWLEDGEMENT

The authors are thankful to the IFTM University, Moradabad and Devsthali Vidyapeeth College of Pharmacy for providing the necessary facilities.

FUNDING

Nil

AUTHORS CONTRIBUTIONS

Experimental work and manuscript writing: Aslam, R. Work designing: Tiwari, V., Tiwari, T. Reviewing the manuscript: Upadhyay, P.

CONFLICT OF INTERESTS

The authors declare no conflict of interest.

REFERENCES

1. Hu FQ, Jiang SP, Du YZ, Yuan H, Ye YQ, Zeng S. Preparation and characterization of stearic acid nanostructured lipid carriers by solvent diffusion method in an aqueous system. Colloids Surf B Biointerfaces. 2005;45(3-4):167-73. doi: 10.1016/j.colsurfb.2005.08.005, PMID 16198092.
2. Müller RH, Radtke M, Wissing SA. Solid lipid nanoparticles (SLN) and nanostructured lipid carriers (NLC) in cosmetic and dermatological preparations. Adv Drug Deliv Rev. 2002;54Suppl 1:S131-55. doi: 10.1016/s0169-409x(02)00118-7, PMID 12460720.
3. Podolak I, Galanty A, Sobolewska D. Saponins as cytotoxic agents: a review. Phytochem Rev. 2010;9(3):425-74. doi: 10.1007/s11101-010-9183-z, PMID 20835386.
4. Jesus M, Martins AP, Gallardo E, Silvestre S. Diosgenin: recent highlights on pharmacology and analytical methodology. J Anal Methods Chem. 2016;2016:4156293. doi: 10.1155/2016/4156293, PMID 28116217.
5. Gan Q, Wang J, Hu J, Lou G, Xiong H, Peng C. The role of diosgenin in diabetes and diabetic complications. J Steroid Biochem Mol Biol. 2020;198:105575. doi: 10.1016/j.jsbmb.2019.105575, PMID 31899316.
6. Fang YW, Zhao JJ, He YZ, Li BG, Xu CJ. Study on the structure of two water-insoluble steroidal saponins of dioscorea. Acta Pharmacol Sin. 1982;17:388-91.
7. Li YM, He BJ, Liu ZY, Jin GS. Study on the water-soluble active ingredient of Dioscorea. J China Med Univ. 1979;8:14-6.
8. Liu CZ, Chang JH, Zhang L, Xue HF, Liu XG, Liu P. Preparation and evaluation of diosgenin nanocrystals to improve oral bioavailability. AAPS PharmSciTech. 2017;18(6):2067-76. doi: 10.1208/s12249-016-0684-y, PMID 27995466.
9. Das S, Ng WK, Tan RBH. Are nanostructured lipid carriers (NLCs) better than solid lipid nanoparticles (SLNs): development, characterizations and comparative evaluations of clotrimazole-loaded SLNs and NLCs? Eur J Pharm Sci. 2012;47(1):139-51. doi: 10.1016/j.ejps.2012.05.010, PMID 22664358.
10. Box GEP, Behnken DW. Some new three-level designs for the study of quantitative variables. Technometrics. 1960;2(4):455-75. doi: 10.1080/00401706.1960.10489912.
11. Chen L, Liu R, Liu C. Scanning electron microscopy: a potentially useful tool for the diagnosis of soft tissue masses. Exp Ther Med. 2013;5(1):172-4.
12. Papadopoulou V, Kosmidis K, Vlachou M. Comparative study of lipid and surfactant self-assembled nanoparticles using a

hydrophilic drug as the active ingredient. Colloids Surf B Biointerfaces. 2014;113:325-32.
13. Ritger PL, Peppas NA. A simple equation for description of solute release I. Fickian and non-fiction release from non-swellable devices in the form of slabs, spheres, cylinders or discs. J Control Release. 1987;5(1):23-36. doi: 10.1016/0168-3659(87)90034-4.
14. Higuchi T. Mechanism of sustained-action medication. Theoretical analysis of rate of release of solid drugs dispersed in solid matrices. J Pharm Sci. 1963;52:1145-9. doi: 10.1002/jps.2600521210, PMID 14088963.
15. Costa P, Sousa Lobo JMS. Modeling and comparison of dissolution profiles. Eur J Pharm Sci. 2001;13(2):123-33. doi: 10.1016/s0928-0987(01)00095-1, PMID 11297896.
16. Das S, Ng WK, Kanaujia P, Kim S, Tan RB. Formulation design, preparation and physicochemical characterizations of solid lipid nanoparticles containing a hydrophobic drug: effects of process variables. Colloids Surf B Biointerfaces. 2011;88(1):483-9. doi: 10.1016/j.colsurfb.2011.07.036, PMID 21831615.
17. Joshi M, Patravale V. Formulation and evaluation of nanostructured lipid carrier (NLC)-based gel of valdecoxib. Drug Dev Ind Pharm. 2006;32(8):911-8. doi: 10.1080/03639040600814676, PMID 16954103.
18. Nerella A, Raju BD, Aruna DM. Formulation, optimization and *in vitro* characterization of letrozole loaded solid lipid nanoparticles. Int J Pharm Sci Drug Res. 2014;6:183-8.
19. Huang ZR, Hua SC, Yang YL, Fang JY. Development and evaluation of lipid nanoparticles for camptothecin delivery: a comparison of solid lipid nanoparticles, nanostructured lipid carriers, and lipid emulsion. Acta Pharmacol Sin. 2008;29(9):1094-102. doi: 10.1111/j.1745-7254.2008.00829.x, PMID 18718178.
20. Gadhave DG, Kokare CR. Nanostructured lipid carriers engineered for intranasal delivery of teriflunomide in multiple sclerosis: optimization and *in vivo* studies. Drug Dev Ind Pharm. 2019;45(5):839-51. doi: 10.1080/03639045.2019.1576724, PMID 30702966.
21. Pokharkar V, Patil Gadhe A, Palla P. Efavirenz loaded nanostructured lipid carrier engineered for brain targeting through intranasal route: *in vivo* pharmacokinetic and toxicity study. Biomed Pharmacother. 2017;94:150-64. doi: 10.1016/j.biopha.2017.07.067, PMID 28759752.
22. Agrawal M, Saraf S, Pradhan M, Patel RJ, Singhvi G, Ajazuddin AA. Design and optimization of curcumin-loaded nano lipid carrier system using box-Behnken design. Biomed Pharmacother. 2021;141:111919. doi: 10.1016/j.biopha.2021.111919, PMID 34328108.
23. Khan BH, Sandhya P. Palbociclib loaded solid lipid nanoparticles by box-Behnken design: solubility enhancement. Int J Pharm Sci Res. 2022;13:1241-50.
24. Schubert MA, Muller Goymann CC. Solvent injection as a new approach for manufacturing lipid nanoparticles-evaluation of the method and process parameters. Eur J Pharm Biopharm. 2003;55(1):125-31. doi: 10.1016/s0939-6411(02)00130-3, PMID 12551713.
25. Schwarz C, Mehnert W, Lucks JS, Muller RH. Solid lipid nanoparticles (SLN) for controlled drug delivery. I. Production, characterization and sterilization. J Control Release. 1994;30(1):83-96. doi: 10.1016/0168-3659(94)90047-7.
26. Lason E, Sikora E, Ogonowski J. Influence of process parameters on properties of nanostructured lipid carriers (NLC) formulation. Acta Biochim Pol. 2013;60(4):773-7. PMID 24432330.
27. Pandey R, Sharma S, Khuller GK. Oral solid lipid nanoparticle-based antitubercular chemotherapy. Tuberculosis (Edinb). 2005;85(5-6):415-20. doi: 10.1016/j.tube.2005.08.009, PMID 16256437.
28. Nikam S, Chavan M. Sharma PH solid lipid nanoparticles: a lipid-based drug delivery. IPP. 2014;2:365-76.
29. Attama AA, Reichl S, Muller Goymann CC. Diclofenac sodium delivery to the eye: *in vitro* evaluation of novel solid lipid nanoparticle formulation using human cornea construct. Int J Pharm. 2008;355(1-2):307-13. doi: 10.1016/j.ijpharm.2007.12.007, PMID 18242022.
30. Kumar P, Bose PP. Targeted delivery of paromomycin to leishmania infected macrophage by hemoglobin tagged nanocarrier. J Appl Pharm. 2016;8:1-6.
31. Zhuang CY, Li N, Wang M, Zhang XN, Pan WS, Peng JJ. Preparation and characterization of vinpocetine-loaded nanostructured lipid carriers (NLC) for improved oral bioavailability. Int J Pharm. 2010;394(1-2):179-85. doi: 10.1016/j.ijpharm.2010.05.005, PMID 20471464.
32. Srawan GY, Madhuri K. Formulation and evaluation of clozapine solid lipid nanoparticles with natural lipid. Drug Discov Ther. 2014;2:18-26.
33. Anuradha K, Senthil KM. Development of lacidipine-loaded nanostructured lipid carriers (NLCs) for bioavailability enhancement. Int J Pharm Res. 2014;2:50-7.
34. Kushwaha AK, Vuddanda PR, Karunanidhi P, Singh SK, Singh S. Development and evaluation of solid lipid nanoparticles of raloxifene hydrochloride for enhanced bioavailability. BioMed Res Int. 2013;2013:584549. doi: 10.1155/2013/584549, PMID 24228255.
35. Nandini PT, Doijad RC, Shivakumar HN, Dandagi PM. Formulation and evaluation of gemcitabine-loaded solid lipid nanoparticles. Drug Deliv. 2015;22(5):647-51. doi: 10.3109/10717544.2013.860502, PMID 24283392.
36. Yang SC, Zhu JB, Lu Y, Liang BW, Yang CZ. Body distribution of camptothecin solid lipid nanoparticles after oral administration. Pharm Res. 1999;16(5):751-7. doi: 10.1023/a:1018888927852, PMID 10350020.
37. Koppel DE. Analysis of macromolecular polydispersity in intensity correlation spectroscopy: the method of cumulants. J Chem Phys. 1972;57(11):4814-20. doi: 10.1063/1.1678153.
38. Joshi G, Tiwari A, Upadhyay P. Optimization and evaluation of piperine loaded herbosomes for their antioxidant and hepatoprotective potential. Asian J Chem. 2022;34(2):383-8. doi: 10.14233/ajchem.2022.23554.
39. Almeida AJ, Runge S, Müller RH. Peptide-loaded solid lipid nanoparticles (SLN): influence of production parameters. International Journal of Pharmaceutics. 1997;149(2):255-65. doi: 10.1016/S0378-5173(97)04885-0.
40. Siekmann B, Westesen K. Thermoanalysis of the recrystallization process of melt-homogenized glyceride nanoparticles. Colloids and Surfaces B: Biointerfaces. 1994;3(3):159-75. doi: 10.1016/0927-7765(94)80063-4.
41. Soma D, Attari Z, Reddy MS, Damodaram A, Koteshwara KBG. Solid lipid nanoparticles of irbesartan: preparation, characterization, optimization and pharmacokinetic studies. Braz J Pharm Sci. 2017;53(1):1-10. doi: 10.1590/s2175-97902017000115012.
42. Varshosaz J, Minayian M, Moazen E. Enhancement of oral bioavailability of pentoxifylline by solid lipid nanoparticles. J Liposome Res. 2010;20(2):115-23. doi: 10.3109/08982100903161456, PMID 19694503.
43. Abdelbary G, Fahmy RH. Diazepam-loaded solid lipid nanoparticles: design and characterization. AAPS PharmSciTech. 2009;10(1):211-9. doi: 10.1208/s12249-009-9197-2, PMID 19277870.
44. Ghanbarzadeh S, Hariri R, Kouhsoltani M, Shokri J, Javadzadeh Y, Hamishehkar H. Enhanced stability and dermal delivery of hydroquinone using solid lipid nanoparticles. Colloids Surf B Biointerfaces. 2015;136:1004-10. doi: 10.1016/j.colsurfb.2015.10.041, PMID 26579567.
45. Malewar N, Avachat M, Pokharkar V, Kulkarni S. Controlled release of ropinirole hydrochloride from a multiple barrier layer tablet dosage form: effect of polymer type on pharmacokinetics and IVIVC. AAPS PharmSciTech. 2013;14(3):1178-89. doi: 10.1208/s12249-013-0009-3, PMID 23897037.
46. Senthil P, Arivuchelvan A, Jagadeeswaran A, Subramanian N, Senthil C, Mekala P. Formulation, optimization and evaluation of enrofloxacin solid lipid nanoparticles for sustained oral delivery. Asian J Pharm Clin Res. 2015;8:231-6.
47. Das S, Chaudhury A. Recent advances in lipid nanoparticle formulations with solid matrix for oral drug delivery. AAPS PharmSciTech. 2011;12(1):62-76. doi: 10.1208/s12249-010-9563-0, PMID 21174180.
48. Singh S, Kamal SS, Sharma A, Kaur D, Katual MK, Kumar R. Formulation and *in vitro* evaluation of solid lipid nanoparticles containing levosulpiride. TONMJ. 2017;4(1):17-29. doi: 10.2174/1875933501704010017.

49. Costa P, Sousa Lobo JM. Modeling and comparison of dissolution profiles. Eur J Pharm Sci. 2001;13(2):123-33. doi: 10.1016/s0928-0987(01)00095-1, PMID 11297896.
50. Dash S, Murthy PN, Nath L, Chowdhury P. Kinetic modeling on drug release from controlled drug delivery systems. Acta Pol Pharm. 2010;67(3):217-23. PMID 20524422.
51. Shetty C, Babubhai S, Pathan I. Development of valdecoxib topical gels-effect of formulation variables on the release of valdecoxib. Int J Pharm Pharm Sci. 2010;2:70-3.
52. Kar N, Chakraborty S, De AK, Ghosh S, Bera T. Development and evaluation of a cedrol-loaded nanostructured lipid carrier system for *in vitro* and *in vivo* susceptibilities of wild and drug-resistant Leishmania donovani amastigotes. Eur J Pharm Sci. 2017;104:196-211. doi: 10.1016/j.ejps.2017.03.046, PMID 28400285.
53. Hao J, Fang X, Zhou Y, Wang J, Guo F, Li F. Development and optimization of solid lipid nanoparticle formulation for ophthalmic delivery of chloramphenicol using a box-Behnken design. Int J Nanomedicine. 2011;6:683-92. doi: 10.2147/IJN.S17386, PMID 21556343.
54. Thakkar HP, Desai JL, Parmar MP. Application of box-Behnken design for optimization of formulation parameters for nanostructured lipid carriers of candesartan cilexetil. J Drug Deliv Sci Technol. 2018;44:431-9.
55. Agrawal M, Saraf S, Pradhan M, Patel RJ, Singhvi G, Ajazuddin AA. Design and optimization of curcumin-loaded Nano lipid carrier system using box-behnken design. Biomed Pharmacother. 2021;141:111919. doi: 10.1016/j.biopha.2021.111919, PMID 34328108.
56. Muller RH, Radtke M, Wissing SA. Solid lipid nanoparticles (SLN) and nanostructured lipid carriers (NLC) in cosmetic and dermatological preparations. Adv Drug Deliv Rev. 2002;54Suppl 1:S131-55. doi: 10.1016/s0169-409x(02)00118-7, PMID 12460720.
57. Patel R, Patel M, Barot B, Patel J, Patel P. Diosgenin: a potent bioactive compound: a review. Orient Pharm Exp Med. 2020;20:203-15.
58. Sharma S, Tandon V, Dehariya M. Diosgenin: a major nutraceutical component from fenugreek. Pharm Lett. 2010;2:369-77.
59. Jain A, Vyas SP. Formulation and characterization of GDL-based artesunate solid lipid nanoparticle. Int J App Pharm. 2023;15:68-74. doi: 10.22159/ijap.2023v15i5.48913.
60. Papadopoulou V, Kosmidis K, Vlachou M. Comparative study of lipid and surfactant self-assembled nanoparticles using a hydrophilic drug as the active ingredient. Colloids Surf B Biointerfaces. 2014;113:325-32.
61. Ibrahim El-Assal M, Samuel D. Optimization of rivastigmine chitosan nanoparticles for neurodegenerative alzheimer; *in vitro* and *ex vivo* characterizations. Int J Pharm Pharm Sci. 2022;14:17-27.
62. Ritger PL, Peppas NA. A simple equation for description of solute release I. Fickian and non-fiction release from non-swellable devices in the form of slabs, spheres, cylinders or discs. J Control Release. 1987;5(1):23-36. doi: 10.1016/0168-3659(87)90034-4.
63. Higuchi T. Mechanism of sustained-action medication. theoretical analysis of rate of release of solid drugs dispersed in solid matrices. J Pharm Sci. 1963;52:1145-9. doi: 10.1002/jps.2600521210, PMID 14088963.
64. Costa P, Sousa Lobo JMS. Modeling and comparison of dissolution profiles. Eur J Pharm Sci. 2001;13(2):123-33. doi: 10.1016/s0928-0987(01)00095-1, PMID 11297896.
65. Rachmawati H, Budiputra DK, Mauludin R. Curcumin nanoemulsion for transdermal application: formulation and evaluation. Drug Dev Ind Pharm. 2015;41(4):560-6. doi: 10.3109/03639045.2014.884127, PMID 24502271.
66. Singh S, Singh J, Singh D, Dubey R. Stable diosgenin loaded solid lipid nanoparticles: a promising system for delivery of anticancer drugs. Chem Phys Lipids. 2018;212:46-54.
67. Zhang J, Wu L, Meng X, Cong Z, Zhang Y, Zhou L. Self-assembly and characterization of hydrophobically modified inulin. J Colloid Interface Sci. 2011;355:533-9.
68. Harde H, Das M, Jain S. Solid lipid nanoparticles: an oral bioavailability enhancer vehicle. Expert Opin Drug Deliv. 2011;8(11):1407-24. doi: 10.1517/17425247.2011.604311, PMID 21831007.
69. Pathak K, Raghuvanshi S. Oral bioavailability: issues and solutions via nanoformulations. Clin Pharmacokinet. 2015;54(4):325-57. doi: 10.1007/s40262-015-0242-x, PMID 25666353.
70. Müller RH, Radtke M, Wissing SA. Nanostructured lipid matrices for improved microencapsulation of drugs. Int J Pharm. 2002;242(1-2):121-8. doi: 10.1016/s0378-5173(02)00180-1, PMID 12176234.
71. Elmowafy M, Al-Sanea MM. Nanostructured lipid carriers (NLCs) as drug delivery platform: advances in formulation and delivery strategies. Saudi Pharm J. 2021;29(9):999-1012. doi: 10.1016/j.jsps.2021.07.015, PMID 34588846.